Journal of Molecular Catalysis B: Enzymatic 99 (2014) 108–113

Contents lists available at ScienceDirect

Journal of Molecular Catalysis B: Enzymatic

journal homepage: www.elsevier.com/locate/molcatb

Highly efficient resolution of mandelic acid using lipase from *Pseudomonas stutzeri* LC2-8 and a molecular modeling approach to rationalize its enantioselectivity

Yan Cao[a], Shanshan Wu[a], Jiahuang Li[b], Bin Wu[a], Bingfang He[a,*]

[a] College of Biotechnology and Pharmaceutical Engineering, Nanjing University of Technology, 30 Puzhunan Road, Nanjing 211816, People's Republic of China

[b] State Key Laboratory of Pharmaceutical Biotechnology, College of Life Sciences, Nanjing University, Nanjing 210093, People's Republic of China

ARTICLE INFO

Article history:
Received 2 August 2013
Received in revised form 31 October 2013
Accepted 31 October 2013
Available online 8 November 2013

Keywords:
Lipase
Pseudomonas stutzeri
Mandelic acid
Resolution
Molecular modeling

ABSTRACT

Mandelic acid, a key precursor of chiral synthons, was successfully acylated in diisopropyl ether. The reaction was catalyzed by the lipase from *Pseudomonas stutzeri* LC2-8, and vinyl acetate was employed as acyl donor. Under the optimized reaction conditions, a resolution of 180 mM (55 g/L) mandelic acid was achieved. (*S*)-*O*-Acetyl mandelic acid was enantioselectivity formed in >99% *ee* at a yield close to the maximum theoretical value for kinetic resolution (50%). The highly substrate tolerable and enantioselective nature of lipase LC2-8 suggests that it is of great potential for the practical resolution of racemic mandelic acid. Additionally, the high enantiopreference of lipase LC2-8 toward (*S*)-mandelic acid in acetylation was also rationalized through molecular docking and molecular dynamics simulations.

1. Introduction

Enantiomers of mandelic acid and their derivatives have been considered as important substances because they are utilized extensively for synthetic purposes as well as in stereochemical investigations. Mandelic acid enantiomers are employed in the resolution of racemic alcohols and amines [1,2]. In addition, (*R*)-mandelic acid is used as a versatile intermediate for preparation of semisynthetic cephalosporins, penicillins, anti-tumor agents and anti-obesity agents [3]. In the last decade, the use of lipases in the enantioselective resolution of racemic mandelic acid for obtaining chiral enantiomers has received considerable attention. Although a high enantiomeric excess (*ee* value) can be obtained in some reports [4–7], the relatively low substrate concentration, usually below 50 mM, restricts its practical application. Therefore, developing the efficient resolution process and improving its space–time yield become imperative.

With the rapid development of computer simulations at present, biomolecular modeling provides a promising way to understand the mechanism and selectivity of enzyme-catalyzed reactions and to guide the modification of enzymes. For example, using docking simulations, Santaniello succeeded in explaining the enantioselectivity of the *Burkholderia cepacia* lipase-catalyzed transesterification of aromatic primary alcohols with vinyl esters with different chain lengths [8]. Based on molecular dynamics simulation, using methyl mandelate as a "model" substrate, Yu's group has successfully shed light on the source of enantioselectivity modified and the trade-off of enantioselectivity and activity in directed evolution of an esterase from *Rhodobacter sphaerioides* [9,10]. Thus, molecular modeling seems to be a good choice to rationalize the enantioselectivity of the lipase-catalyzed acylation of mandelic acid.

Recently, we screened and characterized lipase LC2-8 from *Pseudomonas stutzeri* [11]. This lipase exhibited significant solvent tolerance and good enantioselectivity toward 1-phenylethanol. In the present work, lipase LC2-8 was used in the resolution of mandelic acid, with vinyl acetate as acyl donor (Fig. 1). Lipase LC2-8 showed high substrate concentration tolerance and excellent enantiopreference toward (*S*)-mandelic acid. In addition, we developed a molecular model and explained the strict enantioselectivity of lipase LC2-8 toward mandelic acid.

1.1. Biological and chemical materials

Lipase LC2-8 from *P. stutzeri* LC2-8 was screened and characterized in our previous report [11]. The strain of *P. stutzeri* LC2-8

* Corresponding author. Tel.: +86 25 58139902; fax: +86 25 58139902.
E-mail address: bingfanghe@njut.edu.cn (B. He).

1381-1177/$ – see front matter.
http://dx.doi.org/10.1016/j.molcatb.2013.10.026

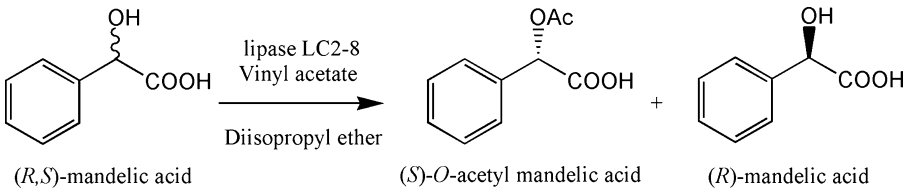

Fig. 1. Resolution of (*R,S*)-mandelic acid catalyzed by lipase LC2-8.

is currently deposited at the China Center for Type Culture Collection (Wuhan, China) with accession number CCTCC M 2010279. The nucleotide sequence of lipase LC2-8 has been assigned a GenBank accession number of JN681265.

Mandelic acid was purchased from Merck (Germany). *p*-Nitrophenyl palmitate (p-NPP) and high-performance liquid chromatography (HPLC)-grade solvents were purchased from Sigma (USA). All other chemicals were of analytical grade.

1.2. Preparation of crude lipase LC2-8

Strain LC2-8 was cultured in lipase-producing medium consisting of (w/v) 1.0% yeast extract, 0.8% glucose, 0.2% K_2HPO_4, 0.05% $MgSO_4{\cdot}7H_2O$, 0.05% (v/v) Triton X-100, and 0.5% (v/v) sunflower oil, at a pH of 8.0. The incubations were carried out with shaking at 180 rpm at 30 °C. After 48 h of growth, the culture supernatant was collected by centrifugation. Chilled acetone was added under magnetic stirring to the crude lipase at 0 °C for 4 h until the ratio was 0.8:1 (v/v). The precipitate was obtained by centrifugation at 10,000 × *g* and 4 °C for 30 min. Finally, the precipitate was air-dried and lipase LC2-8 powder was obtained. The lipase activity was determined using a modified spectrophotometric method with p-NPP as substrate [12].

1.3. Resolution of mandelic acid catalyzed by lipase LC2-8

The resolution of (*R,S*)-mandelic acid was carried out in isopropyl ether containing 300 mM vinyl acetate and 30 mM mandelic acid. The reaction was carried out with shaking at 180 rpm, and was catalyzed by 10 mg/mL (30 U/mL) lipase LC2-8 powder at 30 °C. A control reaction was done by performing the above procedure in the absence of enzyme.

1.4. Enantiomeric analysis of products by HPLC

The concentrations of (*R,S*)-mandelic acid, (*S*)-, and (*R*)-*O*-acetyl mandelic acid were determined by HPLC (Dionex P680) using a Chiracel OD-H column (250 mm × 4.6 mm) and *n*-hexane/isopropanol/TFA (94/6/0.2, v/v/v) as mobile phase, which was introduced at a flow rate of 1 mL/min. The wavelength of the UV detector was set at 228 nm. The enantiomeric excess (ee_p, ee_s) and conversion yield (c) were calculated using the corresponding peak areas:

Enantiomeric excess,

$$ee_p = \frac{[(S)\text{-}O\text{-acetyl mandelic acid}] - [(R)\text{-}O\text{-acetyl mandelic acid}]}{[(S)\text{-}O\text{-acetyl mandelic acid}] + [(R)\text{-}O\text{-acetyl mandelic acid}]}$$

$$ee_s = \frac{[(R)\text{-mandelic acid}] - [(S)\text{-mandelic acid}]}{[(S)\text{-mandelic acid}] + [(R)\text{-mandelic acid}]}$$

Conversion yield [13],

$$c = \frac{ee_s}{ee_s + ee_p}$$

All reported data are averages of experiments performed at least in triplicate.

1.5. Construction of the homology model of lipase LC2-8

Lipase LC2-8 is composed of 311 amino acid residues including a predicted 24-amino acid signal peptide. All computational methods were carried out using DS2.5 (Accelrys Software Inc., San Diego, CA) [14]. A search of the NCBI database was done using the Basic Local Alignment Search Tool (BLAST) [15]. Automated sequence alignment between lipase LC2-8 and the template sequence was carried out. The BLAST search showed significant sequence identity (78.9%) between lipase LC2-8 and *Pseudomonas aeruginosa* lipase (Protein Data Bank (PDB) code: 1EX9) possessing the highest bit score of 450.7. Unanimously, the crystal structure of PAL (resolution 2.5 Å) was selected as the template. The generated structure was improved by subsequent refinement of the loop conformations by assessing the compatibility of an amino acid sequence to known PDB structures using the Protein Health module [14]. The geometry of loop regions was corrected using the Refine Loop. The three-dimensional structure of lipase LC2-8 obtained was further optimized by energy minimization. The steepest-descent method was set at 500 steps for first minimization, and was followed by 1000 steps of the conjugate gradient method. The programs PROCHECK [16] and Profiles-3D [17] were used to validate the accuracy of the refined model of lipase LC2-8.

1.6. Docking and molecular dynamics simulations

It is known that the transesterification mechanism is based on the acylation and deacylation of the catalytic triad of serine, and involves two tetrahedral intermediates. The first intermediate results from the nucleophilic attack of the catalytic serine on the acylating substrate, and forms the acyl–enzyme complex. The second derives from the nucleophilic attack of the acyl acceptor substrate on the acyl–enzyme complex, and leads to the release of the ester product [18]. Therefore, the Ser82 residue is covalently bound to the acyl group in order to mimic the acyl–enzyme complex [8,19,20].

The acylation of Ser82 was constructed using the Build fragment module of DS2.5. All hydrogen atoms were added in their theoretical positions. The catalytic residues Asp228 and His250 were assigned as deprotonated. After all preparations, the acyl–enzyme complex was run through 1000 steps of conjugate gradient energy minimization with the backbone atoms of the enzyme fixed, using the CHARMM force field.

The docking experiment was performed using the protocol of Dock Ligand (LibDock) (Receptor–Ligand Interactions module in DS2.5) [21]. The acyl–enzyme complex was used as receptor and the active site side chain residues were defined as the binding site sphere. The ligands with optimized structures were docked into the active site of the enzyme. The generated conformations were manually analyzed, and the one corresponding to the lowest energy and the highest consensus score was selected for the subsequent energy minimizations.

Considering that the docking algorithm treats the protein as a rigid body, a careful post-docking optimization was carried out on the enzyme–substrate complexes, in order to take into account a potential induced fit effect (little displacements in the protein

Table 1
Effect of organic solvents on the acylation of (*R,S*)-mandelic acid catalyzed by lipase LC2-8.

Solvent	Log *P*	Conversion yield (%)	ee_p (%)
Diisopropyl ether	1.90	49	99
Diethyl ether	0.85	40.5	99
THF	0.5	45.3	95.3

Reactions were carried out in various organic solvents (2 mL) with (*R,S*)-mandelic acid (30 mM), vinyl acetate (300 mM), and lipase LC2-8 (20 mg) at 30 °C for 15 h.

Table 2
Effect of temperature on the acylation of (*R,S*)-mandelic acid catalyzed by lipase LC2-8.

Temperature (°C)	Conversion yield (%)	ee_p (%)
25	49	99
30	49	99
35	49	99
40	51.7	93.4

Reactions were carried out in diisopropyl ether (2 mL) with (*R,S*)-mandelic acid (30 mM), vinyl acetate (300 mM), and lipase LC2-8 (20 mg) at 30 °C for 15 h.

structure due to the presence of the ligand) [20]. The energy minimization consisted of three steps as follows: (1) a fix constraint was applied on the protein backbone and all the remaining parts of the system were tethered with a harmonic restraint; (2) the protein backbone was kept fix, the side chains were kept tethered and the docked ligand was free to move; (3) only the backbone was kept fix, with side chains and the ligands free to move. The Conjugate Gradient algorithm was used in the three steps, with root mean square deviation (*rmsd*) gradients of 0.01, 0.001and 0.0001 kcal mol^{-1} $Å^{-1}$, respectively.

In order to evaluate the dynamics of the docked substrates, further 510 ps MD trajectory was executed on the corresponding complexes with CHARMm force field, adopting a 12 Å nonbound spherical cut-off, using the isothermal-isochoric ensemble (NVT) and with distance-dependent dielectric implicit solvent model, maintaining the backbone fix. In particular, the stability of the essential hydrogen bond interactions and the critical distances for reactivity were verified. The trajectories were divided in 5 ps of heating from 50 to 300 K, 5 ps of equilibration at 300 K and 500 ps of production at 300 K. Frames were registered every 500 fs. Only production phases were considered for analysis.

2. Results and discussion

2.1. Effect of organic solvents and temperatures on the enantioselectivity of resolution

Enzymatic reactions in organic solvent are known to be highly sensitive to the solvent selection, especially in hydrophilic solvent systems. Generally, comparable to the hydrophobic counterparts, the hydrophilic solvents could more easily strip the "essential water" bound to the lipase, which is necessary to preserve the flexibility of the enzyme conformation; this phenomenon deactivates the lipase [22]. However, our previous investigations demonstrated that lipase LC2-8 showed significant stability in both hydrophobic and hydrophilic solvent [11]. Since mandelic acid has poor solubility in hydrophobic solvents, we employed weakly hydrophilic or hydrophilic solvents such as diisopropyl ether, diethyl ether, and tetrahydrofuran (THF) as media for resolution of mandelic acid. As shown in Table 1, diisopropyl ether gave the best result with regard to enantioselectivity (ee_p 99%) and reaction rate (15 h for 49% conversion). When the reaction was carried out in THF, a relatively low *ee* value (95.3%) was obtained. This lower value may be due to the interaction of polar solvent with enzyme that might have resulted in small changes in the lipase active site [23]. Diisopropyl ether was therefore chosen as medium for the resolution of mandelic acid in the subsequent experiments.

In an enzymatic reaction, the temperature significantly influences the activity, enantioselectivity, and stability of a biocatalyst [24,25]. The effect of reaction temperature on enantioselectivity of mandelic acid was investigated. As shown in Table 2, lipase LC2-8 maintained strict enantioselectivity at temperatures between 25 and 35 °C; the ee_p was higher than 99%. With further increase of temperature up to 40 °C, a decrease in enantioselectivity was observed. Generally, at higher temperature, the structure of the enzyme is slightly more flexible compared with its state at low temperature. Therefore, lipase probably loses enantiomeric specificity at high temperature as a result of the increased flexibility [26]. Thus, 35 °C was considered as the optimum temperature for the resolution.

2.2. Effect of substrate molar ratio and mandelic acid concentration on the efficiency of resolution

Many investigators hypothesize that increasing the amount of acyl donor could aid in forming the acyl–enzyme intermediate and accelerate the reaction rate [27]. As Fig. 2 shows, the conversion yield increased with increasing molar ratio of vinyl acetate to (*R,S*)-mandelic acid up to 8:1, and further increase in the molar ratio of two reactants did not significantly increase the conversion yield of mandelic acid. On the other hand, no change in the enantioselectivity of lipase LC2-8 occurred as the substrate molar ratio increased, indicating the rigorous enantioselectivity of lipase LC2-8 toward mandelic acid. Therefore, the optimal substrate molar ratio of vinyl acetate to mandelic acid for the reaction was thought to be 8:1.

A production process with high yield and high conversion is of considerable economic significance. In the actual catalytic process, enzyme activity is frequently inhibited by the existence of its own substrate at relatively high concentrations. The effect of mandelic acid concentration was also investigated. As shown in Fig. 3, although the conversion yield decreased when mandelic acid concentration increased from 30 to 180 mM, the acylation rate of mandelic acid sharply rose even at the same enzyme loading, without effect on the high entantioseletivity of lipase LC2-8. A further increase to higher concentrations of mandelic acid (e.g., 220 mM) led to a dramatic decrease of the conversion rate, presumably via substrate inhibition. After the optimization of enzyme loading (20 mg/mL of final concentration), the conversion yield reached 49.8% with an ee_p of >99% (data not shown).

2.3. Time course of kinetic resolution of mandelic acid

We monitored the time course of the enantioselective acylation of mandelic acid catalyzed by lipase LC2-8 under the optimized conditions. The results show that (*S*)-*O*-acetyl mandelic acid was obtained in 99.8% *ee*, and the conversion reached 49.15% within 15 h (Fig. 4). There are a number of reports on lipase mediated hydrolysis of racemic mandelic acid esters as well as the acylation of racemic mandelic acid [3–7]. Han reported that the enantioselectivity ratio for (*R*)-mandelic acid (*E*) was drastically increased from 29.2 to more than 300 upon immobilization of *Burkholderia* sp. GXU56 lipase, using octyl sepharose CL-4B as support [5]. Yu's group enhanced the enantioselectivity of esterase from *Rhodobacer sphaeroides* in hydrolytic kinetic resolution of methyl mandelate by directed evolution [9]. In contrast, the ability of lipase from *P. stutzeri* LC2-8 to efficiently catalyzed the resolution of (*R,S*)-mandelic acid demonstrates its intrinsic enantioselectivity to mandelic acid. Moreover, the lipase from *Burkholderia ambifaria* YCJ01 reported by our group also displayed a remarkable enantioselectivity toward mandelic acid, while the substrate concentration

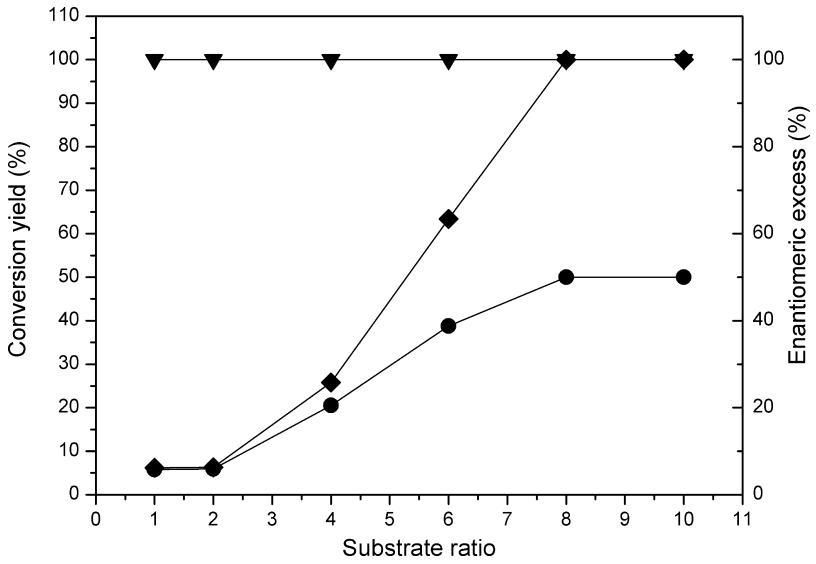

Fig. 2. Effect of substrate mole ratio on the acylation of (*R*,*S*)-mandelic acid catalyzed by lipase LC2-8. Reactions were carried out in diisopropyl ether (2 mL) with lipase LC2-8 (20 mg) at 30 °C for 15 h. The concentration of (*R*,*S*)-mandelic acid was kept constant (30 mmol), whereas the concentration of vinyl acetate was varied from 30 to 300 mM. Symbols: (●) conversion yield; (♦) ee_s; (▼) ee_p.

was about 30 mM [7]. From the viewpoint of practical application, high substrate concentration would be beneficial for practical application of an enzymatic process because it could improve the space–time yield and reduce the cost of product isolation to a large extent. In the present study, the concentration of (*R*,*S*)-mandelic acid reached 180 mM (55 g/L), which is significantly higher than those in other reports which expounded the resolution of mandelic acid with a substrate concentration below 50 mM [3–7]. The highly substrate tolerance and enantioselective nature of lipase LC2-8 suggests that it is of great potential for the practical resolution of racemic mandelic acid.

2.4. Construction of the molecular model and molecular docking to rationalize the enantioselectivity

The calculated Ramachandran plot suggests that 91.97% of the residues in the derived model are either in the most favored or in the additional allowed regions. A model structure of protein with a high percentage of residues in the favored and allowed categories more plausibly represents the folding of the protein. Thus, PROCHECK validates the folding integrity of our model and indicates that the model structure derived from the template (1EX9) is of higher quality in terms of protein folding. The Profile-3D score of the model is 178.23 against 197.15, the maximum expected score. The built model was also evaluated by superimposing the template with the crystal structure; the root-mean-square deviation (*rmsd*) for the superimposition based on C_α atom positions was found to be 0.391 Å. The active site residues were compared and superimposed with the template structure. The conserved catalytic residues (Ser82, Asp228, and His250) in the lipase LC2-8 model have orientations and locations similar to those of the residues in the template (1EX9). The oxyanion hole consists of two residues whose backbone amide protons stabilize the tetrahedral intermediate formed during the reaction mechanism. In lipase LC2-8, the oxyanion hole is probably formed by the main chain nitrogens of Met16 and His83. His83 is next to the catalytic Ser, whereas Met16 is located in a loop after β-strand 3, next to a Gly residue.

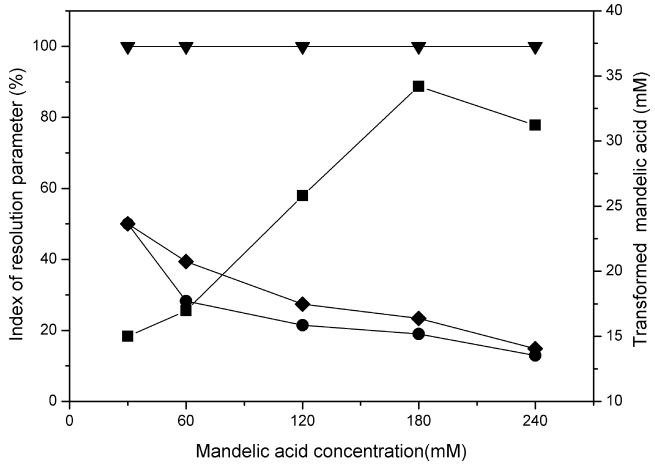

Fig. 3. Effect of mandelic acid concentration on the acylation of (*R*,*S*)-mandelic acid catalyzed by lipase LC2-8. Reactions were carried out in diisopropyl ether (2 mL) with lipase LC2-8 (20 mg) at 30 °C for 15 h. The molar ratio of vinyl acetate to mandelic acid was kept constant (8:1). Symbols: (●) conversion yield; (♦) ee_s; (▼) ee_p; (■) the amount of transformed mandelic acid.

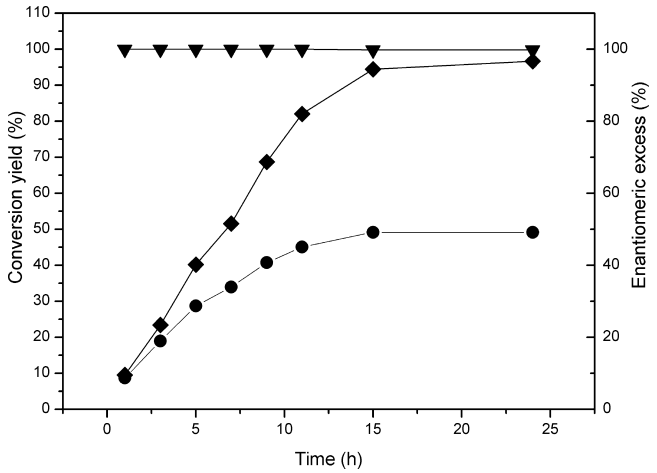

Fig. 4. Time course of resolution of (*R*,*S*)-mandelic acid catalyzed by lipase LC2-8. Reaction was carried out in 2 mL diisopropyl ether with (*R*,*S*)-mandelic acid (180 mM), vinyl acetate (1440 mM), and lipase LC2-8 (40 mg) at 30 °C. Symbols: (●) conversion yield; (♦) ee_s; (▼) ee_p.

On the basis of the modeled structure, molecular docking of (*R*,*S*)-mandelic acid to lipase LC2-8 was undertaken. Some reports indicate that protein conformational rearrangements may be needed for better ligand affinity, but if the protein distortion is too extensive, the orientation of some essential residues may be disturbed, leading to loss of activity [20]. In our case, the conformational changes of lipase LC2-8 were minimal (*rmsd* values about 0.9 Å) after docking. The docking results show that both enantiomers could access the catalytic center of lipase LC2-8, while the acetate oxygen atom (namely Ace:O) of vinyl acetate orienting to Ser82 forms hydrogen bonds with the backbone NH of Met16 and His83 in the oxyanion hole (Fig. 5) in both complexes. These hydrogen bonds may help to stabilize transition-state complex for the second tetrahedral intermediate. The alcohol hydroxyl of (*S*)-mandelic acid is located close to the active site, with distances of 2.929 Å from Ace:C and 2.56 Å from His250:N_ε (Fig. 5 and Table 3). These results are in accordance with the required conditions [28] for the complex to be productive (i.e., the respective distances to catalytic His and Ser are <4 Å), suggesting that acylation may occur on the alcohol hydroxyl of (*S*)-mandelic acid. In the case of (*R*)-mandelic acid, it distorts the orientation of the imidazole ring of the catalytic histidine, thereby breaking the hydrogen bond between the imidazole and the oxygen of the substrate (Fig. 5) and preventing the protonation of His250. The alcohol hydroxyl is localized at distances of 5.362 and 4.57 Å from the Ace:C and the His250:N_ε, respectively. Such distances relative to the histidine and the acetate exceed the maximal distance criterion for acylation that allows proton transfer and nucleophilic attack. Therefore, forming the second tetrahedral intermediate between (*R*)-mandelic acid and acetyl-lipase is difficult.

Table 3
Distances of hydroxyl groups of mandelic acid from the N_ε atom of His250 (His250:N_ε) of lipase LC2-8 and acetate carbonyl carbon (Ace:C) of vinyl acetate orienting to Ser82 after docking.

Complexes	d_{H-N} (Å)	d_{O-C} (Å)
S	2.56	2.929
R	4.57	5.362

It is well known that applying molecular dynamics on complexes obtained by docking would be efficient to refine the models, accounting for the flexibility of both receptor and ligand [29]. To complement our study of docking experiments, we carried out 510 ps of molecular dynamics simulations on the docking complexes after optimization. The stability of the lipase LC2-8 structure all along the trajectory was monitored with the RMSD of the backbone atoms referring to the initial structure of the protein. During the MD production phase, the *rmsd* values were about 0.8–1.5 Å, indicating the protein did not undergo significant distortions and the systems were stable throughout simulations. The essential hydrogen bonds between the acetate carbonyl oxygen of the serine-bound acetate (Ace:O) and the oxyanion hole residues, Met16: HN and His83: HN, were present in most of trajectory frames, which indicated the acetate was in a catalytically competent orientation. The trajectories were also analyzed basing on the mandelic acid alcohol hydroxyl from the catalytic residue His250 and the

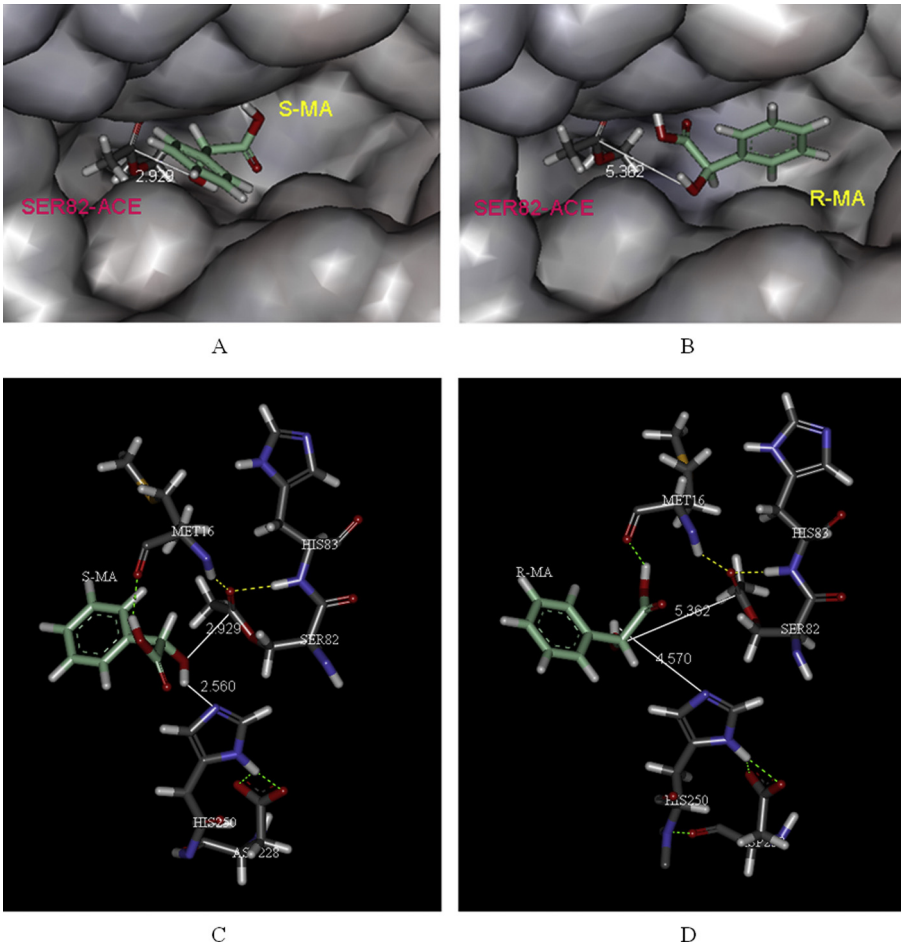

Fig. 5. Models of the binding between lipase LC2-8 and (*R*,*S*)-mandelic acid obtained from the LibDock approach. (A) The (*S*)-mandelic acid–lipase LC2-8 complex. (B) The (*R*)-mandelic acid–lipase LC2-8 complex. (C) The hydrogen bonding interactions of (*S*)-mandelic acid with catalytic residues and key residues of lipase LC2-8. (D) The hydrogen bonding interactions of (*R*)-mandelic acid with catalytic residues and key residues of lipase LC2-8.

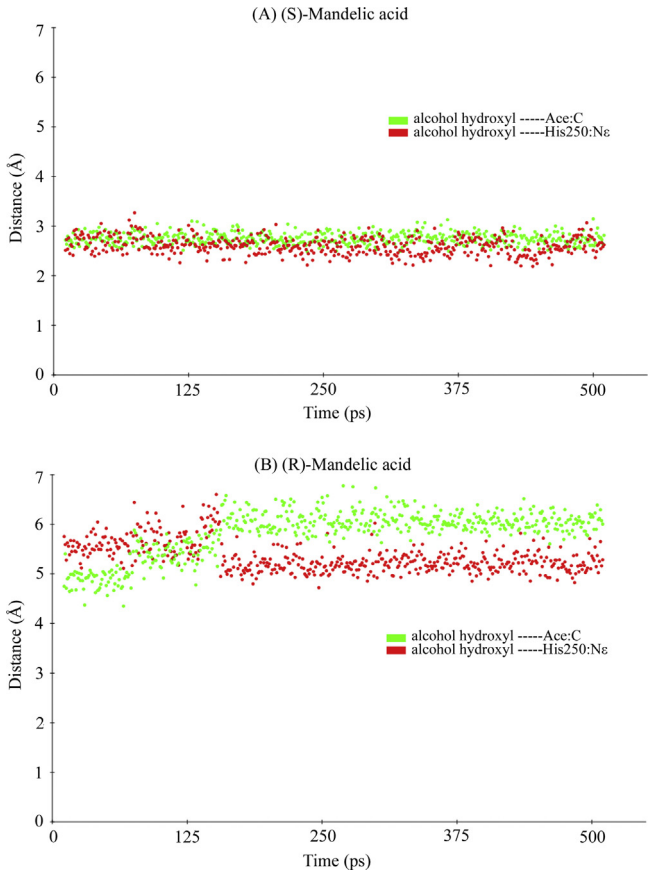

Fig. 6. The distances from mandelic acid alcohol to the Ace:C atom and the His250:Nε atom along the trajectory.

serine-bound acetate. Results were shown in Fig. 6. The alcohol hydroxyl of (*S*)-mandelic acid maintained close to the catalytic residues at distances inferior to 3.2 Å all along the trajectories. For (*R*)-mandelic acid, the alcohol hydroxyl was too far from the catalytic residues (about 4.5–6.5 Å). These results from molecular dynamics simulations on the docking complexes reinforce our conclusions about enantioselectivity of lipase LC2-8 toward mandelic acid.

3. Conclusion

In this paper, lipase LC2-8 demonstrated excellent enantioselective acylation toward (*S*)-mandelic acid and afforded a conversion yield of 49.15% and an ee_p value of 99%. The reaction concentration of (*R*,*S*)-mandelic acid reached 180 mM (55 g/L), which is markedly higher than previously reported. In addition, the mechanism of catalysis of the resolution of mandelic acid with high enantioselectivity by lipase LC2-8 was analyzed. Molecular docking was used to obtain the models of interaction between (*R*,*S*)-mandelic acid and lipase LC2-8. The results reasonably explain the high enantioselectivity of lipase LC2-8 in the chiral resolution of mandelic acid. The analysis of molecular dynamics simulations on the docking complexes reinforces the conclusions about enantioselectivity of lipase LC2-8 toward mandelic acid. These results may contribute to the design and engineering of other lipases, especially those with improved enantioselectivity, for chiral resolution.

Acknowledgements

Financial supports for this research from the National Program on Key Basic Research Project (2011CB710800) and the National High Technology Research and Development Key Program of China (2012AA022200). We also acknowledge the support of the projects funded by PCSIRT (IRT1066) and PADD.

References

[1] J.K. Whitesell, D. Reynolds, J. Org. Chem. 48 (1983) 3548–3551.
[2] S.P. Zingg, E.M. Arnett, A.T. McPhail, A.A. Bothner By, W.R. Gilkerson, J. Am. Chem. Soc. 110 (1988) 1565–1580.
[3] G.D. Yadav, P. Sivakumar, Biochem. Eng. J. 19 (2004) 101–107.
[4] J.M. Palomo, G. Fernandez Lorente, C. Mateo, C. Ortiz, R. Fernandez Lafuente, J.M. Guisan, Enzyme Microb. Technol. 31 (2002) 775–783.
[5] H.N. Wei, B. Wu, Appl. Biochem. Biotechnol. 149 (2008) 79–88.
[6] N. Queiroz, M.G. Nascimento, Tetrahedron Lett. 43 (2002) 5225–5227.
[7] C.J. Yao, Y. Cao, S.S. Wu, S. Li, B.F. He, J. Mol. Catal. B: Enzym. 85–86 (2013) 105–110.
[8] E. Santaniello, S. Casati, P. Ciuffreda, G. Meroni, A. Pedretti, G. Vistoli, Tetrahedron: Asymmetry 20 (2009) 1833–1836.
[9] J.B. Ma, L. Wu, F. Guo, J.L. Gu, X.L. Tang, L. Jiang, J. Liu, J.H. Zhou, H.W. Yu, Appl. Microbiol. Biotechnol. 97 (2013) 4897–4906.
[10] F. Guo, H.M. Xu, H.N. Xu, W.H. Yu, Appl. Microbiol. Biotechnol. 97 (2013) 3355–3362.
[11] Y. Cao, Y. Zhuang, C.J. Yao, B. Wu, B.F. He, Biochem. Eng. J. 64 (2012) 55–60.
[12] U.K. Winkler, M. Stuckmann, J. Bacteriol. 138 (1979) 663–670.
[13] Y.H. Zhang, Z.Y. Li, C.J. Yuan, Tetrahedron Lett. 43 (2002) 3247–3249.
[14] Accelrys Software Inc., Discovery Studio Modeling Environment, Release 2.5, Accelyrs Software Inc., San Diego, 2009.
[15] S.F. Altschul, T.L. Madden, A.A. Schäffer, J. Zhang, Z. Zhang, W. Miller, D.J. Lipman, Nucleic Acids Res. 25 (1997) 3389–3402.
[16] R.A. Laskowski, M.W. MacArthur, D.S. Moss, J.M. Thornton, J. Appl. Crystallogr. 26 (1993) 283–291.
[17] J. Bowie, R. Luthy, D. Eisenberg, Science 253 (1991) 164–170.
[18] A.B.C. Simas, A.A.T.D. Silva, A.G. Cunha, R.S. Assumpção, L.V.B. Hoelz, B.C. Neves, T.C. Galvão, R.V. Almeida, M.G. Albuquerque, D.M.G. Freire, R.B. de Alencastro, J. Mol. Catal. B: Enzym. 70 (2011) 32–40.
[19] B. Christelle, B.D.O. Eduardo, C. Latifa, M. Elaine-Rose, M. Bernard, R.-H. Evelyne, G. Mohamed, E. Jean-Marc, H. Catherine, J. Biotechnol. 156 (2011) 203–210.
[20] E.B. De Oliveira, C. Humeau, L. Chebil, E.R. Maia, F. Dehez, B. Maigret, M. Ghoul, J.M. Engasser, J. Mol. Catal. B: Enzym. 59 (2009) 96–105.
[21] S.N. Rao, M.S. Head, A. Kulkarni, J.M. LaLonde, J. Chem. Inf. Model. 47 (2007) 2159–2171.
[22] A.M. Klibanov, Trends Biotechnol. 15 (1997) 97–101.
[23] D.H. Yu, Z. Wang, L.F. Zhao, Y.M. Cheng, S.G. Cao, J. Mol. Catal. B: Enzym. 48 (2007) 64–69.
[24] A. Wolff, L. Zhu, Y.W. Wong, A.J.J. Straathof, J.A. Jongejan, J.J. Heijnen, Biotechnol. Bioeng. 62 (1999) 125–134.
[25] S.Y. Han, Z.Y. Pan, D.F. Huang, M. Ueda, X.N. Wang, Y. Lin, J. Mol. Catal. B: Enzym. 59 (2009) 168–172.
[26] D.Y. Kwon, Y.J. Hong, S.H. Yoon, J. Agric. Food Chem. 48 (2000) 524–530.
[27] G. Yang, J.P. Wu, G. Xu, L.R. Yang, Appl. Microbiol. Biotechnol. 81 (2009) 847–853.
[28] C. Palocci, M. Falconi, S. Alcaro, A. Tafi, R. Puglisi, F. Ortuso, M. Botta, L. Alberghina, E. Cernia, J. Biotechnol. 128 (2007) 908–918.
[29] H. Alonso, A.A. Bliznyuk, J.E. Gready, Med. Res. Rev. 26 (2006) 531–568.